# Equilibrium and Nonequilibrium Contributions to the $(p, n)$ Cross Sections of Y, Nb, and Ta†

S. M. Grimes, J. D. Anderson, B. A. Pohl, J. W. McClure, and C. Wong
*Lawrence Radiation Laboratory, Livermore, California 94550*
(Received 19 April 1971)

The neutron spectra produced by the $^{89}Y(p,n)^{89}Zr$, $^{93}Nb(p,n)^{93}Mo$, and $^{181}Ta(p,n)^{181}W$ reactions have been measured at five angles between 15 and 135° for proton energies between 7.8 and 14.8 MeV. It is concluded that the data at low bombarding energies are consistent with a compound-nuclear-reaction mechanism. A constant-temperature level density for energies below the neutron binding energy is found to be appropriate for the residual nuclei $^{89}Zr$, $^{93}Mo$, and $^{181}W$, with nuclear temperatures $\theta = 0.70$, 0.68, and 0.54 MeV, respectively.

For bombarding energies above 10 MeV contributions from noncompound processes appear and at 14.8 MeV these are comparable in magnitude to those produced by compound-nuclear $(p,n)$ reactions. On the basis of the angular distributions and the bombarding-energy dependence the relative fraction of the noncompound cross section due to direct and to pre-equilibrium reaction mechanisms is estimated.

The extracted average doorway-state width varies from 350 keV near $A = 90$ to about 1 MeV for $A \sim 180$.

## I. INTRODUCTION

A recent study[1] of the $^{51}V(p, n)^{51}Cr$ and $^{59}Co(p, n)^{59}Ni$ reactions has yielded estimates of 160 keV for the doorway-state widths. Careful examination of the dependence of the neutron spectra on bombarding energy and residual excitation made it possible to divide the neutron spectra into equilibrium and nonequilibrium portions. Comparison of this latter component with theoretical predictions[2-4] enabled a further separation into direct and pre-equilibrium contributions to be made. It was suggested that nuclei with lower nuclear temperatures might yield better information on the pre-equilibrium reaction mechanism, because the equilibrium contribution to a given region of the spectrum would decrease more rapidly with increasing bombarding energy, making the pre-equilibrium contribution relatively more prominent.

Measurements of the neutron spectra produced in the $^{89}Y(p, n)^{89}Zr$, $^{93}Nb(p, n)^{93}Mo$, and $^{181}Ta(p, n)^{181}W$ reactions were carried out both to test this prediction and to investigate the dependence on $A$ of the pre-equilibrium state width.

The statistical theory[5] predicts that the differential cross section for emission of particles of energy $E$ integrated over angle can be related to the level density $\rho(U)$ of the residual nucleus as follows:

$$\sigma(\epsilon) \propto \epsilon \sigma_c(\epsilon) \rho(U), \tag{1}$$

where $\epsilon$ is the channel kinetic energy and $\sigma_c(\epsilon)$ is the capture cross section for the inverse reaction at an energy $\epsilon$. Although many experiments have yielded results consistent with the statistical theory, other measurements[6,7] have indicated that the continuum spectra cannot be described entirely by Eq. (1). Specifically, the level-density parameters obtained from such measurements were functions of the bombarding energy as well as the residual excitation. The logical explanation[6,7] for this behavior is that nonequilibrium processes also contributed to the continuum spectra. A specific model[2-4] for such a mechanism has been proposed and both the bombarding energy and residual excitation dependence were calculated as functions of the single-particle level density. Thus, experimental information on the above energy dependences of pre-equilibrium contributions provides a test of the assumptions of the current model.

## II. THEORY

The formal treatment of intermediate structure by Feshbach, Kerman, and Lemmer[8] contains the basic concepts required to analyze pre-equilibrium emission, i.e., the continuum decay of "doorway" states. In this basic treatment the cross sections are calculated from the resonance parameters of the intermediate states rather than the various level densities themselves. The extention to the level-density case is carried out as in the statistical compound-nucleus case.

Feshbach, Kerman, and Lemmer[8] have shown that the pre-equilibrium cross section for the process $(\alpha, \beta)$ is

$$\sigma_{\alpha\beta} = \sigma_{\alpha\,\mathrm{abs}} \Gamma_{\beta\,\mathrm{con}} / \Gamma_{\mathrm{int}}, \tag{2}$$

where $\sigma_{\alpha\,\mathrm{abs}}$ is the absorption cross section for particle $\alpha$, $\Gamma_{\beta\,\mathrm{con}}$ is the width of the intermediate

state for emission of particle $\beta$, and $\Gamma_{\rm int}$ is the total width of the intermediate state. The width $\Gamma_K$ for emission of particle $\beta$ leaving the nucleus in a particular state can be shown to be[4]

$$\Gamma_K = \frac{D}{2\pi}\sum_l (2l+1)T_l\,, \tag{3}$$

where $D$ is the average spacing between states and $T_l$ is the transmission coefficient for angular momentum $l$. If the inverse capture cross section is introduced in place of the sum in Eq. (3) and if the width to all residual states is summed, this expression becomes[9]

$$\Gamma_{\beta\,\rm con}dE = \frac{(2S+1)m\sigma_{\beta\,\rm inv}}{\pi^2\hbar^2\rho_{\rm int}(E^*)}E\rho'(E_0-E)dE\,, \tag{4}$$

where $m$ and $S$ are the mass and spin of the emitted particle, respectively, $\rho'(U)$ is the density of states in the residual nucleus which can be reached by emission from an intermediate state, and $\rho_{\rm int}(E^*)$ is the density of intermediate states in the compound nucleus at an excitation energy $E^*$. If Eq. (4) is substituted into Eq. (2), the following result is obtained:

$$\sigma_{\alpha\beta}(E)dE = \frac{(2S+1)m}{\pi^2\hbar^2}\,\frac{\sigma_{\alpha\,\rm abs}(E_0)\sigma_{\beta\rm inv}(E)E\rho'(E_0-E)}{\rho_{\rm int}(E^*)\Gamma_{\rm int}}\,. \tag{5}$$

Equation (5) is a model-independent expression and does not depend on the nature of the intermediates states. In practice, use of Eq. (5) to evaluate intermediate widths requires an assumption as to the form of $\rho_{\rm int}(E^*)$, while $\rho'(U)$ can be determined from the shape of the emission spectrum. The form of Eq. (5) is completely analogous to the compound-nucleus case where the relevant level densities and widths refer to the particle-hole or compound states, respectively.

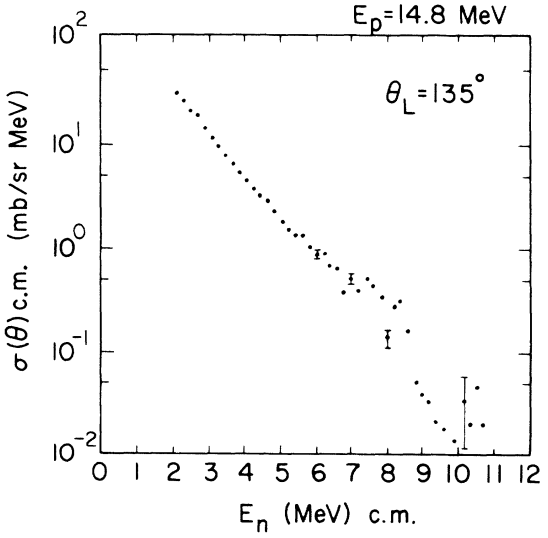


FIG. 1. The differential cross section for the $^{89}$Y$(p,n)$-$^{89}$Zr reaction as a function of center-of-mass neutron energy. The bombarding energy was 14.8 MeV and the laboratory angle was 135°. Indicated errors are statistical only.

## III. EXPERIMENTAL PROCEDURE

Neutron spectra from the $^{89}$Y$(p,n)^{89}$Zr, $^{93}$Nb$(p,n)^{93}$Mo, and $^{181}$Ta$(p,n)^{181}$W reactions for angles at 30° intervals from 15 to 135° were obtained with the experimental technique described previously.[10] The Livermore 2.3-m variable energy cyclotron produced protons with energies from 7.8 to 14.8 MeV. Neutrons resulting from the bombardment of self-supporting targets of Y, Nb, and Ta were detected in NE213 scintillators with the neutron energy determined by the time of flight over a 10.8-m flight path. A linear bias eliminated pulses produced by recoil protons with energies less than 1.6 MeV and $\gamma$-produced background was reduced by utilizing pulse-shape discrimination. A typical $(p,n)$ spectrum is shown in Fig. 1.

TABLE I. Nuclear temperatures for $^{89}$Zr, $^{93}$Mo, and $^{181}$W.

| $E_p$ (MeV) | $U$ range (MeV) | 15° | 45° | 75° | 105° | 135° |
|---|---|---|---|---|---|---|
| | | $^{89}$Y$(p,n)^{89}$Zr | | | | |
| 10.0 | 2–4 | 0.74 | 0.68 | 0.69 | 0.65 | 0.68 |
| 12.3 | 2–4 | 1.04 | 0.98 | 0.88 | 0.93 | 0.84 |
| | 4–6.5 | 0.81 | 0.71 | 0.74 | 0.69 | 0.70 |
| 14.8 | 2–4 | 2.04 | 1.98 | 1.72 | 1.58 | 1.34 |
| | 4–6.5 | 1.29 | 1.30 | 1.22 | 1.12 | 0.97 |
| | 6.5–9 | 0.79 | 0.74 | 0.72 | 0.75 | 0.72 |
| | | $^{93}$Nb$(p,n)^{93}$Mo | | | | |
| 8.7 | 3.5–5.5 | 0.68 | 0.64 | 0.67 | 0.69 | 0.67 |
| 10.0 | 3.5–6 | 0.73 | 0.70 | 0.69 | 0.68 | 0.69 |
| 12.3 | 3.5–6 | 0.88 | 0.86 | 0.90 | 0.87 | 0.83 |
| | 6–8 | 0.83 | 0.75 | 0.74 | 0.78 | 0.73 |
| 14.0 | 3.5–6 | 1.03 | 1.17 | 1.09 | 0.96 | 0.94 |
| | 6–8 | 1.18 | 1.18 | 1.08 | 1.04 | 0.96 |
| | | $^{181}$Ta$(p,n)^{181}$W | | | | |
| 8.0 | 2–5 | 0.49 | 0.55 | 0.52 | 0.53 | 0.54 |
| 8.7 | 2–5 | 0.55 | 0.61 | 0.52 | 0.54 | 0.57 |
| 9.6 | 2–4 | 0.62 | 0.53 | 0.60 | 0.59 | 0.51 |
| | 4–6.7 | 0.60 | 0.58 | 0.50 | 0.54 | 0.57 |
| 10.0 | 2–4 | 0.86 | 0.75 | 0.68 | 0.62 | 0.60 |
| | 4–6.7 | 0.62 | 0.59 | 0.57 | 0.56 | 0.53 |
| 10.4 | 2–4 | 0.91 | 0.81 | 0.80 | 0.77 | 0.74 |
| | 4–6.7 | 0.69 | 0.63 | 0.62 | 0.62 | 0.64 |
| 11.7 | 2–6.7 | 1.12 | 1.18 | 1.11 | 1.03 | 1.05 |
| 12.3 | 2–6.7 | 1.25 | 1.37 | 1.41 | 1.20 | 1.18 |
| 14.8 | 2–6.7 | 1.71 | 1.42 | 1.35 | 1.31 | 1.26 |

## IV. DATA REDUCTION AND ANALYSIS

### A. Level Densities and Pre-Equilibrium Emissions Below the Neutron Binding Energy

The technique of analysis was identical to that described in a previous paper.[1] The continuum portion of the $(p, n)$ spectra was analyzed by calculating the "channel" cross section:

$$\sigma(\theta, \epsilon) = \frac{A+1}{A}\sigma(\theta, E_n)_{\text{c.m.}} , \tag{6}$$

where $A$ is the mass number of the residual nucleus, $\epsilon = [(A+1)E_n/A]_{\text{c.m.}}$ is the channel kinetic energy, and $\sigma(\theta, E_n)_{\text{c.m.}}$ is the center-of-mass cross section for the reaction. If the capture cross section $\sigma_c(\epsilon)$ is assumed to be constant, the $\sigma(\theta, \epsilon)/\epsilon$ will be proportional to the level density of the residual nucleus. In general, if pre-equilibrium or direct contributions are also present, additional terms[1] of the form $U^n$ will also be needed to fit the spectrum. Because the coefficients of the various terms are expected to have different dependences on bombarding energy, the shape of the continuum spectrum will change as a function of bombarding energy, unless only one reaction mechanism is involved.

Such changes can be observed in Table I and in Figs. 2–4, which show the spectra for the $^{89}$Y$(p, n)$,

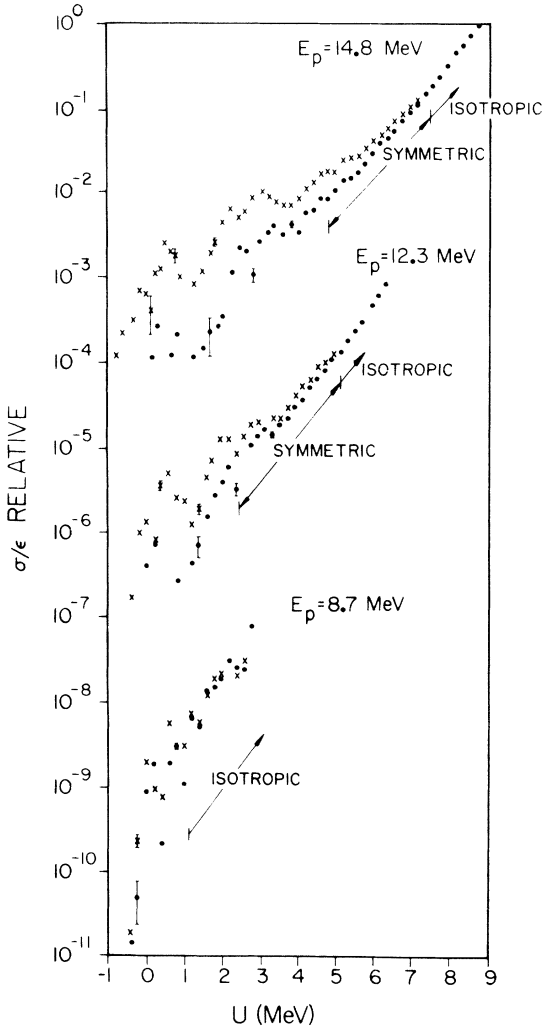


FIG. 2. Neutron spectra from the $^{89}$Y$(p,n)^{89}$Zr reaction at three bombarding energies. The points labeled × are at 15°; those labeled • are at 135°. Indicated on each spectrum are the regions in which the angular distribution was symmetric or isotropic.

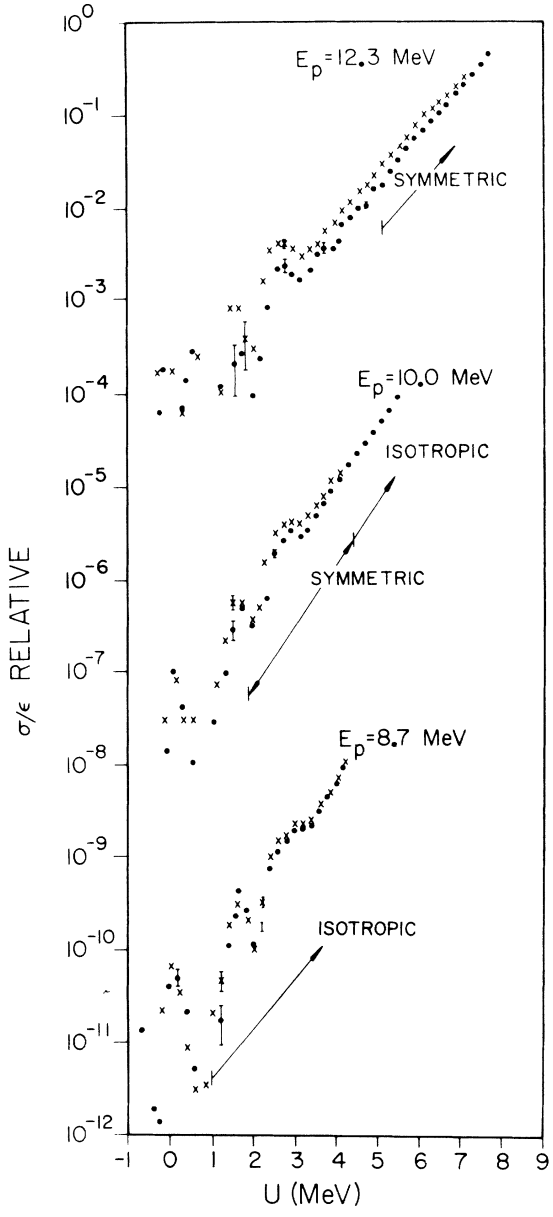


FIG. 3. Same as Fig. 2 for the $^{93}$Nb$(p,n)^{93}$Mo reaction.

$^{93}$Nb($p$, $n$), and $^{181}$Ta($p$, $n$) reactions, respectively. At low energies ($E_p \leq 10$ MeV) the continuum spectra were either symmetric or isotropic, while for higher energies a forward-peaked angular distribution was observed.

Backward angle (135°) spectra for a number of different bombarding energies are shown in Figs. 5–7. The lines drawn through the low-energy spectra for the Y($p$, $n$) and Nb($p$, $n$) reactions were obtained by connecting the data points for the appropriate 10.0-MeV spectrum; as can be seen, the same shape is also observed at lower energies. It is concluded that the ($p$, $n$) reaction mechanism is essentially entirely compound nuclear in this energy region for these two reactions. The Ta spectra are consistent with a completely compound-nuclear-reaction mechanism only below bombarding energies of 9.6 MeV.

In each case a constant-temperature level-density form is seen to be appropriate for excitation energies between 3 MeV and the neutron binding energy. The nuclear temperatures obtained were 0.70, 0.68, and 0.54 MeV for $^{89}$Zr, $^{93}$Mo, and $^{181}$W, respectively. Below 3 MeV, the level densities show too much structure to be characterized with a temperature, although the average slope is not significantly different from that above 3 MeV.

At higher energies the continuum spectra were fit with an expression of the form

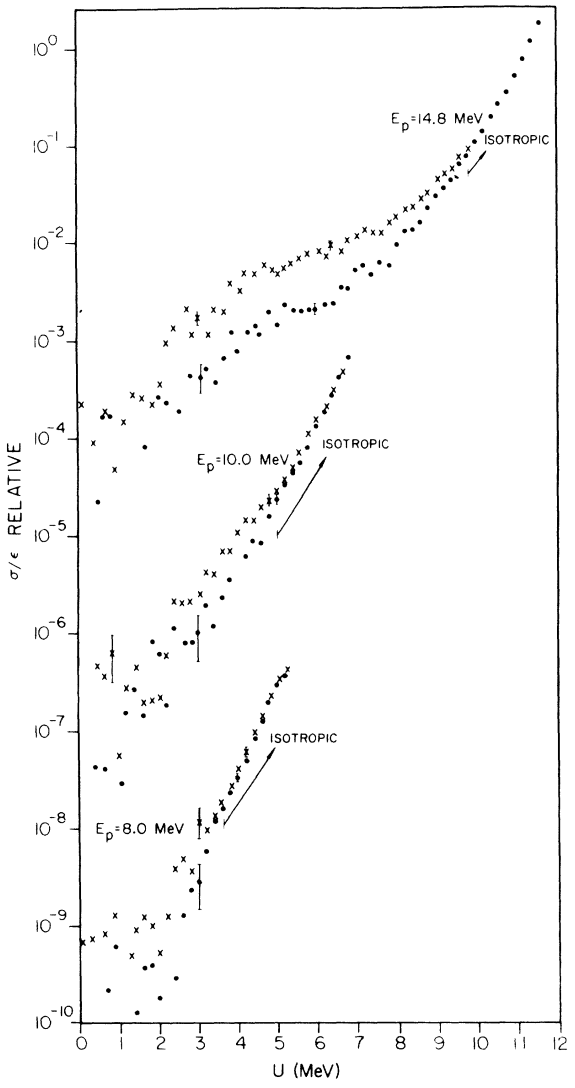


FIG. 4. Same as Fig. 2 for the $^{181}$Ta($p$,$n$)$^{181}$W reaction, except that the points marked × are at 45°.

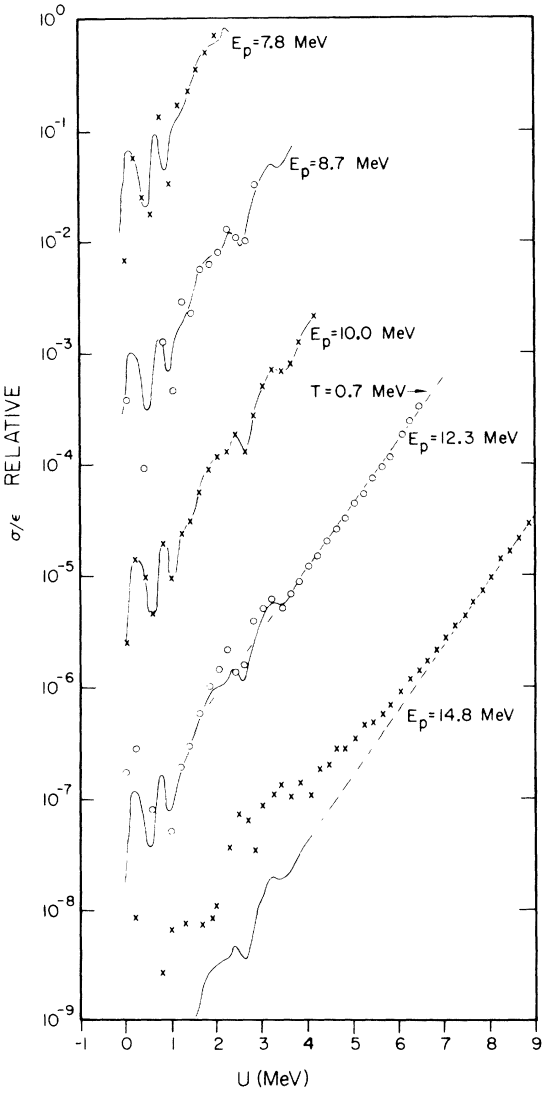


FIG. 5. Comparison of 135° neutron spectra produced in the $^{89}$Y($p$,$n$)$^{89}$Zr reaction. The solid line was obtained by connecting the data points in the 10.0-MeV spectrum and is extended to higher energies with the best-fit constant-temperature form.

$$\sigma(\theta, \epsilon)/\epsilon = A\rho(U) + BU^n . \quad (7)$$

The nuclear temperatures determined at lower energy were used in a constant-temperature level-density form for $\rho(U)$ and the best-fit values of $A$ and $B$ were calculated for $0 \leq n \leq 6$. Figure 8 shows two examples of the quality of fit obtained for the best-fit value of $n$, and Fig. 9 displays the changes in fit as a function of $n$. As can be seen, the best-fit value of $n$ could be determined to within a range of 1 or 2. The $^{181}$Ta$(p, n)^{181}$W data at 14.8 MeV showed essentially no equilibrium contribution but in all other cases nonzero values for $A$ were obtained.

To test the uniqueness of the fits, an alternative form was tried

$$\sigma(\theta, \epsilon)/\epsilon = BU^n + CU^m , \quad (8)$$

where $0 \leq n \leq 3$, $n+1 \leq m \leq 6$. This parametrization can represent the spectrum over a limited range, but the fits showed systematic deviations from the data for high $U$. In no case did Eq. (8) provide a better fit than Eq. (7); for the 14.8-MeV Ta$(p, n)$ data, where as already mentioned a very small value for $A$ was obtained, the fits were equally good.

The best-fit values of $n$ obtained with Eq. (7) are listed in Table II. A value of 1[1] would be expected for either a direct or a pre-equilibrium reaction mechanism if the single-particle level spacing is independent of energy and if higher-order

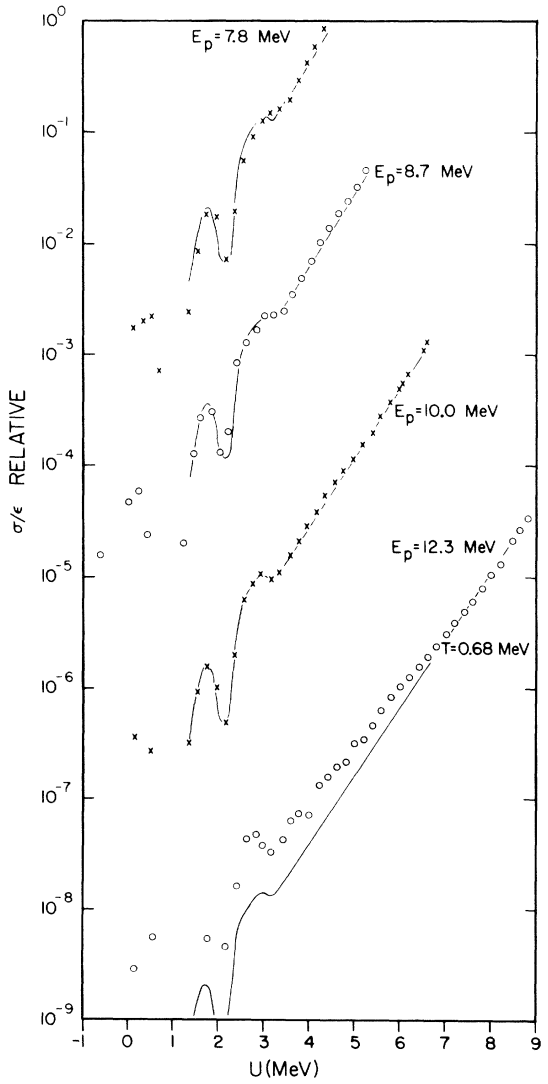


FIG. 6. Same as Fig. 5 for the $^{93}$Nb$(p,n)^{93}$Mo reaction.

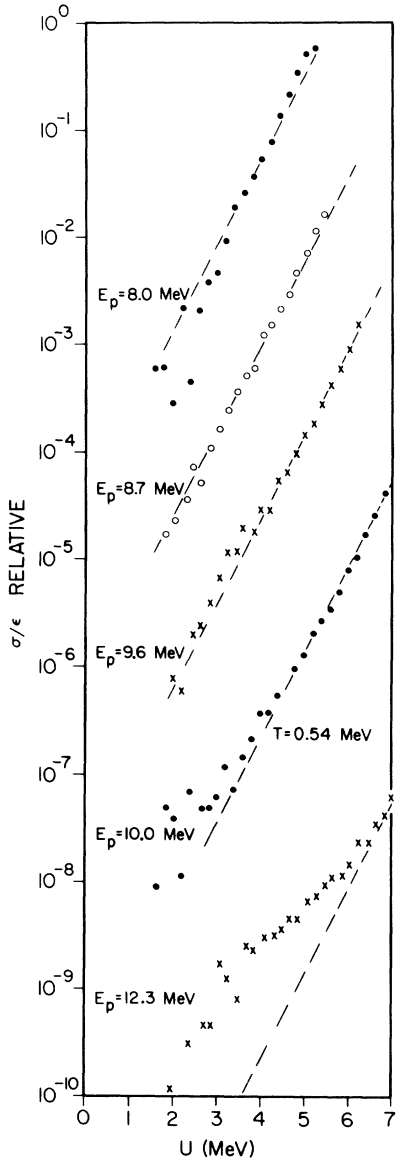


FIG. 7. Same as Fig. 5 for the $^{181}$Ta$(p,n)^{181}$W reaction, except that the dashed line is the best-fit constant-temperature form obtained at low bombarding energies.

terms in $U$ can be ignored. In spite of this prediction, the values 2, 3, and 5 are obtained for the $^{89}$Y$(p, n)^{89}$Zr, $^{181}$Ta$(p, n)^{181}$W, and $^{93}$Nb$(p, n)^{93}$Mo reactions, respectively. The fits were originally carried out in the energy region between $U = 2$ MeV and the smaller of the two quantities: the neutron binding energy and the highest energy for which data were available. It was subsequently found that reducing the limits to a region as small as $4 \leq U \leq 6$ MeV did not change the best-fit values of $n$ obtained, although it reduced the difference between the best and worst fits. Thus, the magnitudes obtained for $n$ are not due to a local anomaly, but are characteristic of excitation energies below the binding energy for these nuclei. Possible explanations for the large $n$ values will be presented in Sec. IV. From these fits the dependence of $A$ and $B$ on angle and bombarding energy were also obtained.

If the term $Ae^{U/T}$ represents the equilibrium contribution, an isotropic or symmetric [11] angular dependence for $A(\theta)$ would be expected. Since $B(\theta)$ may in general contain contributions from both direct and pre-equilibrium processes, a forward-peaked angular distribution for $B(\theta)$ would be predicted.

As can be seen from Fig. 10, these predictions were verified. Also shown for comparison in Fig. 10 is the 14.8-MeV Y$(p, n)$ angular distribution for neutrons leaving $^{89}$Zr in the ground and first excited states. Since these residual states should have more overlap with the $^{89}$Y ground state than would be expected for higher excited states, it is reasonable to assume that the angular distribution to these states should be more characteristic of direct reactions than would the nonequilibrium contributions to continuum states. These two tran-

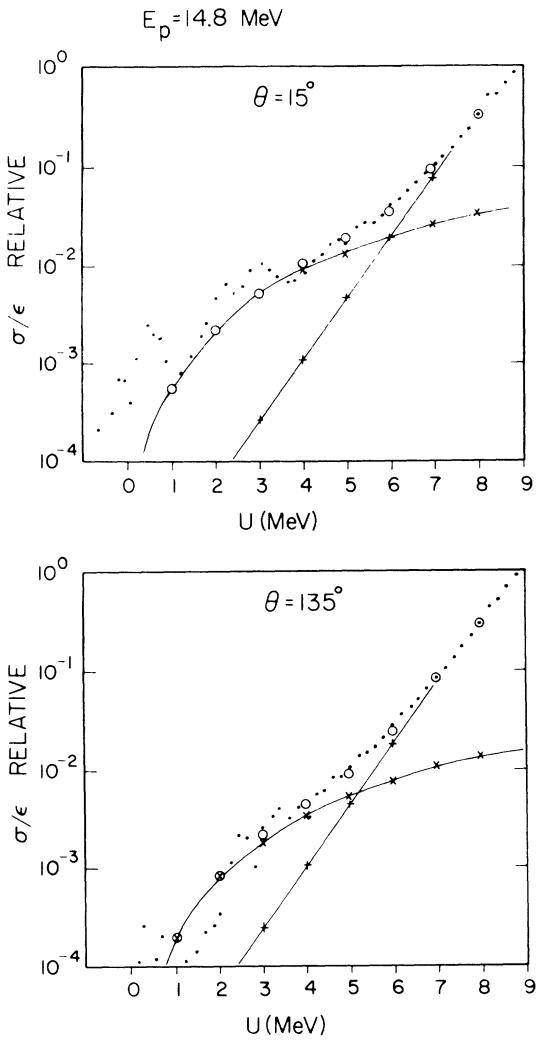


FIG. 8. Fits of the form $Ae^{U/T} + BU^n$ to the 14.8-MeV $^{89}$Y$(p, n)^{89}$Zr neutron spectrum. Both a forward and a backward angle are shown. The experimental spectrum is denoted with •, the $Ae^{U/T}$ term contribution (equilibrium) with +, the $BU^n$ contribution (nonequilibrium) with ×, and the sum $Ae^{U/T} + BU^n$ with ○.

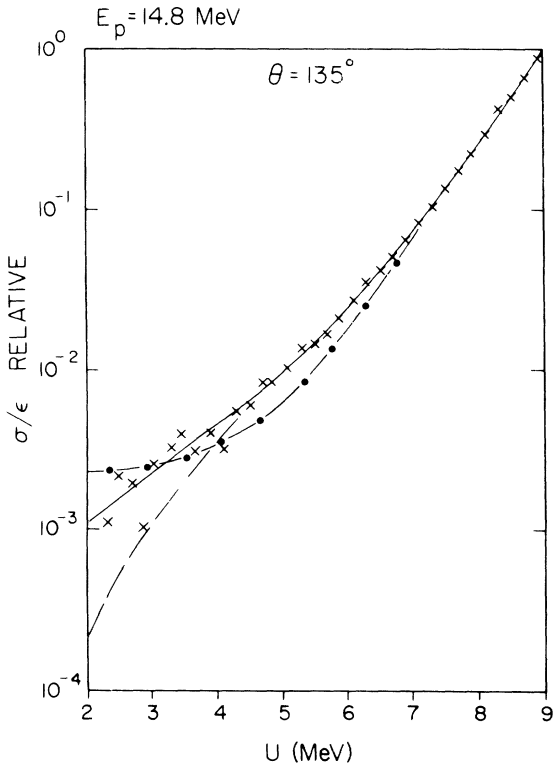


FIG. 9. Variation of the quality of fit to the neutron spectrum of the expression $Ae^{U/T} + BU^n$ as a function of $n$. The 14.8-MeV $^{89}$Y$(p, n)^{89}$Zr spectrum at 135° is the example shown. The experimental spectrum is denoted ×, and the best-fit spectra for $m = 0$, 2, and 4 are denoted by the dot dash, the solid line, and the dashed line, respectively.

sitions are $\frac{1}{2}^-$ to $\frac{9}{2}^+$ and $\frac{1}{2}^-$ to $\frac{1}{2}^-$ for the ground and first excited states, respectively; the combination of two such different transitions would be expected to be more representative of the continuum angular distribution for direct processes than would either individually. Inspection of Fig. 10 indicates that adding an isotropic component to the form obtained for the first two levels can reproduce roughly the shape observed for the nonequilibrium portion. With this decomposition one estimates equal contributions to the nonequilibrium cross section from direct and pre-equilibrium processes.

### B. Level Densities Above the Neutron Binding Energy

Above the neutron binding energy the level density cannot be obtained from the shape of the evaporation spectrum directly, because of the presence of $(p, 2n)$ neutrons in the spectrum. An alternative technique proposed by Ericson,[12] can be used to extend the level-density measurements beyond this point. For a reaction which proceeds to a given final state through the compound nucleus, the energy dependence of the cross section is determined primarily by the level densities in the residual nuclei reached by particle emission. The Coulomb barrier will inhibit competition from nuclei reached by charged-particle emission; thus, the energy dependence of the cross section for these nuclei will be determined primarily by the level density of the nucleus reached by neutron emission.

The following relation is obtained by Weisskopf and Ewing[13]:

$$\sigma_{\alpha\beta}(E, E_1) = \frac{E_1 \sigma_{\beta\,\mathrm{inv}}(E_1)\sigma_{\alpha\ \mathrm{abs}}(E)}{\int_0^{E+Q} E'\sigma_{\beta\,\mathrm{inv}}(E')\rho(E+Q-E')dE'}, \quad (9)$$

TABLE II. Best-fit $n$ values.

| $E_p$ (MeV) | 15° | 45° | 75° | 105° | 135° |
|---|---|---|---|---|---|
| | | $^{89}Y(p, n)^{89}Zr$ | | | |
| 12.3 | 1 | 1, 2 | 1 | 1, 2 | 2 |
| 14.8 | 2 | 1, 2 | 2 | 2 | 3 |
| | | $^{93}Nb(p, n)^{93}Mo$ | | | |
| 10.0 | 3, 4 | 3 | 3, 4 | 4 | 3–5 |
| 12.3 | 5 | 5 | 5 | 4, 5 | 5 |
| 14.0 | 5 | 5, 6 | 4, 5 | 5 | 5, 6 |
| | | $^{181}Ta(p, n)^{181}W$ | | | |
| 10.4 | 3, 4 | 3 | 3 | 3, 4 | 3 |
| 11.7 | 4 | 3 | 3 | 3, 4 | 4 |
| 12.3 | 3 | 3 | 2 | 3 | 3 |
| 14.8 | 2 | 3 | 3 | 3 | 3 |

where $\sigma_{\alpha\beta}(E, E_1)$ is the cross section for a compound-nuclear reaction initiated by particle $\alpha$ with energy $E$ leading to the emission of particle $\beta$ with energy $E_1$, $\sigma_{\alpha\ \mathrm{abs}}(E)$ is the absorption cross section for particle $\alpha$ at an energy $E$, $\sigma_{\beta\,\mathrm{inv}}(E')$ is the absorption cross section for particle $\beta$ at an energy $E'$, $\rho(U)$ is the level density of the residual nucleus, and $Q$ is the $Q$ value for the reaction $(\alpha, \beta)$. If the level density is assumed to have a constant-temperature energy dependence and if $\sigma_{\mathrm{inv}}(E')$ is assumed to be a constant, the following results:

$$\frac{\sigma_{\alpha\beta}(E, E_1)}{E_1} = \frac{\sigma_{\alpha\ \mathrm{abs}}(E)}{\int_0^E E'Ce^{(E+Q-E')/T}dE'} = \frac{\sigma_{\alpha\ \mathrm{abs}}(E)}{T^2\rho(E+Q)}. \quad (10)$$

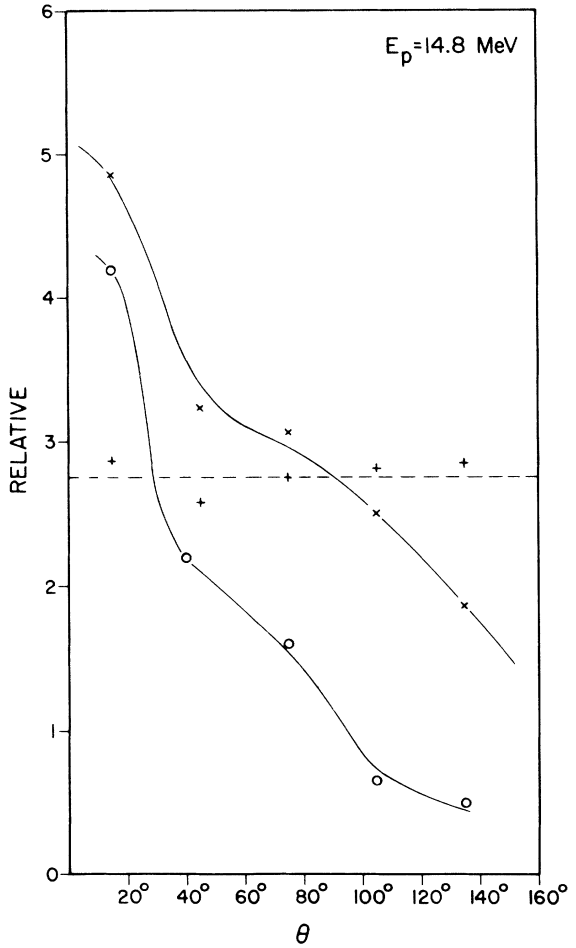


FIG. 10. Dependence of $A(E, \theta)$ and $B(E, \theta)$ on $\theta$ for the $^{89}Y(p, n)^{89}Zr$ reaction at 14.8 MeV. The $A(E, \theta)$ values (equilibrium) are denoted + and the estimated angular distribution is denoted by the dashed line. Contributions from the $B(E, \theta)$ term are labeled with an × and those from the $(p, n_0 + n_1)$ groups with a ○. In each case the approximate angular distribution is indicated with a solid line.

Since the right side of Eq. (10) does not depend on $E_1$, the cross sections to a number of levels, divided in each case by the outgoing energy, can be summed to obtain

$$\sum_{i=1}^{N} \frac{\sigma_{\alpha\beta}(E, E_i)}{E_i} = \frac{N\sigma_{\alpha\,\mathrm{abs}}(E)}{T^2\rho(E+Q)}, \tag{11}$$

where $N$ is the number of levels included in the analysis. The technique used in separating the equilibrium and nonequilibrium contributions to the spectra yields a parametrization of the equilibrium portion in the form

$$[\sigma(E_1)/E_1]_{\mathrm{equil.}} = Ae^{U/T}, \tag{12}$$

where $A$ is a function of bombarding energy. Comparison of Eqs. (11) and (12) shows that

$$\rho(E+Q) \propto \sigma_{\alpha\,\mathrm{abs}}(E)/A(E) . \tag{13}$$

Thus, the energy dependence of the level density for energies above the neutron binding energy can be obtained from the variation of $A(E)$ with bombarding energy.

The results obtained for $^{89}$Zr, $^{93}$Mo, and $^{181}$W are shown in Figs. 11–13. Potential parameters proposed by Becchetti and Greenlees[14] were used to calculate the proton absorption cross sections. Since only the relative values of $\sigma_{\alpha\,\mathrm{abs}}(E)$ are needed, the results are not particularly sensitive to the potential parameters used. The optical-model potential of Hodgson[15] yielded absorption cross sections which differed by 30–40% from those of Becchetti and Greenlees, but because the energy dependence is similar, use of the Hodgson cross sections would change the relative values of the level density by less than 10%. Each $A(E)$ value yields a relative measurement of the level density at the excitation energy corresponding to the incident center-of-mass energy minus the $Q$ value for the $(p, n)$ reaction; thus, there is some overlap between the region covered with this technique and that obtained directly from the spectral shape. In each case, the energy dependence extracted using the two techniques agrees within errors. The constant-temperature level-density form is found to be appropriate for excitation energies up to 10 MeV. For the appropriate choice of $a$, the excitation-energy dependence of the usual Fermi-gas form $\{\rho(U) = [1/(U-\delta)^2]e^{2[a(U-\delta)]^{1/2}}\}$ does not differ appreciably over an energy range of a few MeV from that of the constant-temperature form; as has been pointed out by Maruyama,[16] the level densities for certain nuclei can be fit with either form over a limited energy range. The present measurements indicate that the constant-temper-

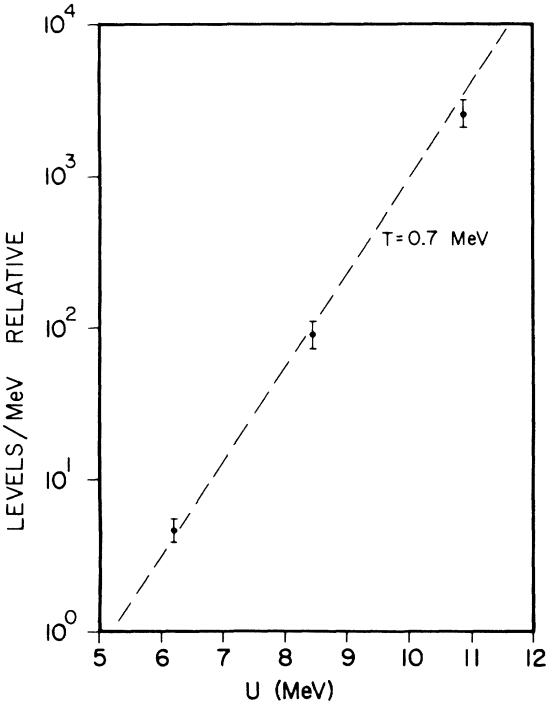


FIG. 11. Level density of $^{89}$Zr obtained from the bombarding energy dependence of $A(E, \theta)$. The dashed line represents the form obtained for energies below the neutron binding energy from the neutron spectral shape.

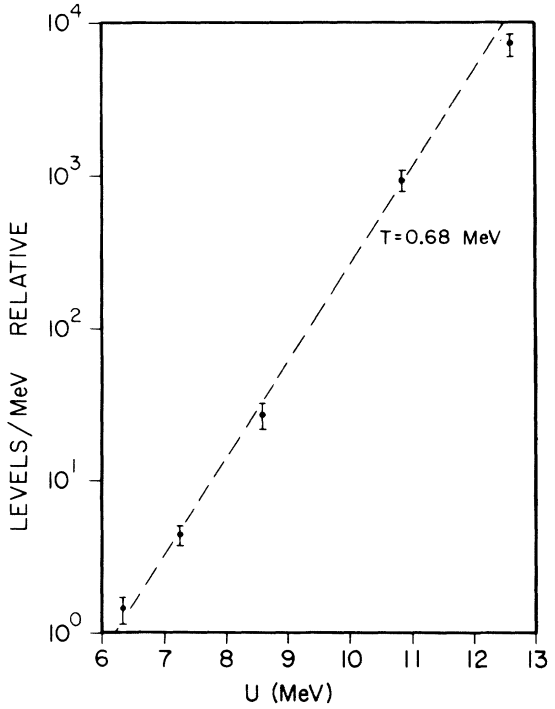


FIG. 12. Level density of $^{93}$Mo obtained from the bombarding energy dependence of $A(E, \theta)$. The dashed line represents the form obtained for energies below the neutron binding energy from the neutron spectral shape.

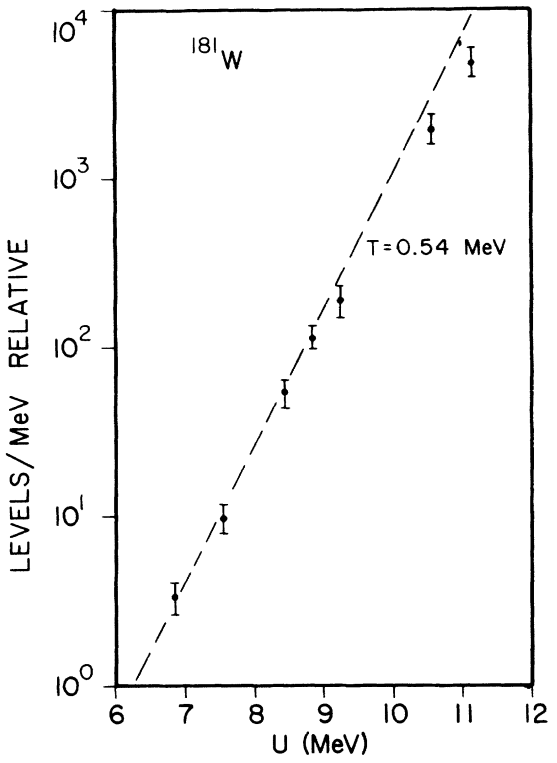


FIG. 13. Level density of $^{181}$W obtained from the bombarding energy dependence of $A(E,\theta)$. The dashed line represents the form obtained for energies below the neutron binding energy from the neutron spectral shape.

ature energy dependence is observed over a larger range than is consistent with a Fermi-gas form. Changes in temperature are observed above 10 MeV and it is felt that these represent the transition to a Fermi-gas energy dependence at higher excitation energies.

### C. Intermediate-Level Widths

Application of the results of Williams[4] and Feshback, Kerman, and Lemmer[8] yields a relation between the pre-equilibrium cross section and the width of the pre-equilibrium state from which decay has occurred.

Solving Eq. (5) for $\Gamma_{\rm int}$, the following result is obtained:

$$\Gamma_{\rm int} = \frac{(2S+1)\sigma_{\rm abs} m \sigma_{\rm cap} \rho_{n-1}(U)}{\pi^2 \hbar^2 \rho_n(E^*)[\sigma_{\rm pe}(\epsilon)/\epsilon]}, \qquad (14)$$

where $\sigma_{\rm abs}$ is the absorption cross section in the entrance channel, $\sigma_{\rm cap}$ is the inverse capture cross section (exit channel), $m$ is the mass of the emitted particle, $E^*$ is the excitation energy in the compound system, and $\rho_n(E^*)$ is the density of $n$-exciton states at an energy $E^*$. The above expression, although it contains $\epsilon$, the energy of the emitted particle, and $U$, the excitation energy of the residual nucleus, does not depend on either of these quantities, because of the proportionality of $\rho_{n-1}(U)$ and $\sigma_{\rm pe}(\epsilon)/\epsilon$. Values for $\Gamma_{\rm int}$ obtained from this relation are shown in Table III. The single-particle level spacing ($g = 6a/\pi^2$) necessary for calculating the level densities was obtained from the relation $a = \frac{1}{8}A$, yielding values of 7 for Zr and Mo and 14 for W. The uncertainty in these widths is substantial, primarily because of the difficulty in estimating the fraction of the nonequilibrium cross section due to direct processes. The estimate of equal direct and pre-equilibrium cross section is uncertain by at least 50%. As can be seen from Table III, the values for $\Gamma_{\rm int}$ are approximately 300 keV for $A$ near 90 and about 1 MeV for $A$ near 180. An earlier determination[1] of $\Gamma_{\rm int}$ yielded a value of 160 ± 80 keV for $A$ near 55.

### D. Relative Magnitude of Equilibrium and Nonequilibrium Cross Sections

The analysis described in Sec. III A provides a parametrization of the spectra in the form

$$\sigma/\epsilon = Ae^{U/T} + BU^n. \qquad (15)$$

Because of the linear bias on the detector, neutrons with energies less than 1.6 MeV were not detected in this experiment. Thus, total cross sections for neutron production cannot be extracted directly from the data.

If the parametrization expressed in Eq. (15) is assumed to be valid over the entire energy range of the neutron spectrum, the integral of the expression will yield the neutron-production cross section, including those parts due to equilibrium and nonequilibrium processes. For higher bombarding energies, all of the neutrons corresponding to $(p,n)$ events will have energies above the detector bias and thus the $(p,n)$ cross sections can be obtained directly. For these cases, the integral was extended beyond the neutron binding energy to the maximum possible excitation energy (zero neutron energy), to provide a value for the sum of the $(p,n)$ and $(p,2n)$ cross sections. If, as is expected for these nuclei, cross sections for charged-particle emission from the compound nu-

TABLE III. Intermediate-resonance widths.

| Nucleus | Compound-nucleus excitation (MeV) | Intermediate-resonance width (keV) |
|---|---|---|
| $^{90}$Zr | 20.5 | 240 ± 120 |
| | 23 | 320 ± 160 |
| $^{94}$Mo | 20.8 | 340 ± 170 |
| | 22.5 | 660 ± 330 |
| $^{182}$W | 19.1 | 610 ± 305 |
| | 21.6 | 1400 ± 700 |

cleus are small, the above sum should be approximately equal to the reaction cross section. This comparison provides an additional approximate test of the appropriateness of the parametrization of Eq. (15), although possible discrepancies could result from changes in the parameters of the level-density formula for high $U$ or variations in the inverse capture cross section for low neutron energies.

The results of these calculations are shown in Table IV. In all cases, the sum of $(p, n)$ and $(p, 2n)$ cross sections is approximately equal to the reaction cross section calculated with the Becchetti parameters. The integral of the $Ae^{U/T}$ term yields more cross section than the integral of the $BU^n$ term, a result consistent with the conclusion that the damping width of the doorway state into more complicated states is much larger than that to the continuum. If the limit of integration is chosen to be the neutron binding energy, approximate values for the equilibrium and pre-equilibrium contributions to the $(p, n)$ cross section can be obtained; as can be seen, essentially all of the $^{181}$Ta$(p, n)^{181}$W cross section is due to nonequilibrium processes at 14.7 MeV, as are substantial portions of the $^{89}$Y$(p, n)^{89}$Zr and $^{93}$Nb$(p, n)^{93}$Mo cross sections. These calculations depend on the assumption that a second neutron will be emitted where this is energetically possible; because of competition from $\gamma$ decay, this represents only a lower limit for the $(p, n)$ cross section. Table IV also presents values of the ratio $\Gamma_{con}/\Gamma_{int}$, the (neutron) width to the continuum divided by the total width of the intermediate states. Since to first order the incoming proton will produce a neutron particle-hole state as often as a proton particle-hole state, on the average three times as many protons as neutrons will be in excited states. The Coulomb barrier will inhibit proton emission relative to neutron emission; nonetheless, it is expected that the proton width would be somewhat larger than the neutron width.

## V. DISCUSSION

### A. Level Densities

Previous determinations of the level-density parameters of nuclei studied in the present work are listed in Table V. The level density of $^{93}$Mo has been studied by Bramblett and Bonner[17] and by Wong *et al.*[18] Comparison of the Bramblett and Bonner results with the present measurements is difficult because the former study is restricted to excitation energies below 4 MeV, while the present measurements indicate that for excitation energies less than 3 MeV considerable structure is present in the level density. They also find that a constant-temperature form fits the data, but ob-

TABLE IV. Equilibrium and nonequilibrium neutron cross sections.

| Target | $E_p$ (MeV) | Equilibrium cross section (mb) $\sigma(p, n)$ | Equilibrium cross section (mb) $\sigma(p, n+2n)$ | Nonequilibrium cross section (mb) $\sigma(p, n)$ | Nonequilibrium cross section (mb) $\sigma(p, n+2n)$ | $\Gamma_{con}/\Gamma_{int}$ |
|---|---|---|---|---|---|---|
| $^{89}$Y | 10.0 | 800 ± 150 | ... | ... | ... | ... |
| | 12.3 | 1250 ± 200 | ... | 67 ± 20 | ... | 0.03 ± 0.01 |
| | 14.8 | 540 ± 150 | 1620 ± 400 | 88 ± 30 | 100 ± 40 | 0.03 ± 0.01 |
| $^{93}$Nb | 8.7 | 760 ± 150 | ... | ... | ... | ... |
| | 10.0 | 800 ± 200 | 1100 ± 350 | 66 ± 15 | 70 ± 30 | 0.03 ± 0.01 |
| | 12.3 | 75 ± 25 | 1000 ± 350 | 75 ± 25 | 200 ± 80 | 0.1 ± 0.03 |
| | 14.0 | 16 ± 5 | 1700 ± 800 | 36 ± 15 | 170 ± 80 | 0.05 ± 0.04 |
| $^{181}$Ta | 8.7 | 77 ± 20 | 110 ± 30 | ... | ... | ... |
| | 10.0 | 36 ± 10 | 330 ± 140 | 6 ± 3 | 9 ± 5 | 0.015 ± 0.01 |
| | 10.4 | 30 ± 10 | 580 ± 300 | 9 ± 5 | 15 ± 10 | 0.015 ± 0.01 |
| | 11.7 | 6 ± 2 | 900 ± 400 | 15 ± 5 | 37 ± 15 | 0.02 ± 0.01 |
| | 12.3 | 2 ± 1 | 800 ± 400 | 15 ± 5 | 43 ± 15 | 0.03 ± 0.01 |
| | 14.8 | ... | ... | 20 ± 8 | 70 ± 30 | ... |
| $^{51}$V [a] | 12.3 | 750 ± 100 | 1040 ± 200 | 40 ± 20 | 43 ± 25 | 0.02 ± 0.01 |
| | 13.2 | 460 ± 100 | 990 ± 300 | 50 ± 20 | 64 ± 40 | 0.03 ± 0.01 |
| | 14.7 | 180 ± 50 | 925 ± 350 | 90 ± 40 | 120 ± 60 | 0.07 ± 0.03 |
| $^{59}$Co [a] | 12.3 | 520 ± 100 | 810 ± 200 | 42 ± 20 | 46 ± 25 | 0.03 ± 0.01 |
| | 13.2 | 320 ± 100 | 740 ± 350 | 30 ± 15 | 33 ± 20 | 0.02 ± 0.01 |
| | 14.7 | 100 ± 40 | 820 ± 350 | 40 ± 15 | 63 ± 30 | 0.04 ± 0.02 |

[a] Data of Ref. 1.

tain a temperature of 0.57 MeV. The results of Wong *et al.*[18] indicate that the level density of $^{93}$Mo has a Fermi-gas form between excitation energies of 3 and 8 MeV; the parameters they obtain for the fit result in a variation of the nuclear temperature between 0.7 and 0.86 over this range, in excellent agreement with the 15° $^{93}$Mo temperatures quoted in Table I. It is now evident that the Fermi-gas dependence observed in Ref. 18 for $^{93}$Mo was due to neglect of nonequilibrium contributions.

The level density of $^{181}$W has also been measured by Holbrow and Barschall,[19] using the $^{181}$Ta($p$, $n$)-$^{181}$W reaction. They find that the shape of the evaporation spectrum changes quite rapidly with proton energy and obtain temperatures of 0.64, 0.70, and 0.78 MeV at bombarding energies of 8, 9, and 10 MeV, respectively. This trend is consistent with that observed in the present measurements (see Table I) and is attributed to the presence of nonequilibrium processes. These temperatures are systematically somewhat higher than those obtained in the present measurements. The explanation for this discrepancy is not clear, although the small cross sections for the ($p$, $n$) reaction on Ta make the results more sensitive to the background subtraction than is the case for the other elements studied.

The level densities for all three nuclei measured in the present study have been obtained previously by Borchers, Wood, and Holbrow.[20] Again, their results could not be reconciled with the traditional equilibrium assumption, because of a dependence of the level density on bombarding energy as well as residual excitation. The values for the nuclear temperature obtained at the lowest bombarding energies are in reasonably good agreement with the present results.

Verbinski and Burris[21] have measured the ($p$, $n$ + $2n$) spectra produced by 18-MeV proton bombardment of Ta. They quote a value of 1.04 MeV for the average temperature of $^{180}$W and $^{181}$W. The equation derived by LeCouteur and Lang[22] was used to obtain this temperature from the $2n$ portion of the spectrum; as will be discussed later, there is some indication that the $2n$ spectrum is not accurately described by this relation, which might account for the discrepancy between the temperature obtained by Verbinski and Burris and that determined in the present measurement.

Level densities for neighboring nuclei have been measured by Maruyama,[16] Owens and Towle,[23] Thomson,[24] Plattner *et al.*,[25] Sobottka *et al.*,[26] and Mathur *et al.*[27] The level-density forms obtained by Maruyama for Y and Nb with the ($n$, $n'$) reaction could be fit with either a Fermi-gas or constant-temperature form; the values for the temperature were about 0.7 MeV, in excellent agreement with the present measurements. The same technique was used by Thomson to obtain level-density parameters for Nb, Ta, and W. He ob-

TABLE V. Level-density parameters.

| Nucleus | Reference | Method | Bombarding energy | $U$ range | $a$ (MeV$^{-1}$) | $T$ (MeV) |
|---|---|---|---|---|---|---|
| $^{89}$Y | 16 | ($n$,$n'$) | 2–7.5 | 2–7.5 | 13.5–21.7 | 0.63–0.84 |
| | 27 | ($n$,$n'$ + $2n$) | 14 | | 13.3 | 0.93 |
| $^{89}$Zr | 20 | ($p$,$n$) | 9–12 | 2–8 | 11 | 0.7–1.0 |
| | Present work | ($p$,$n$) | 7.8–14.8 | 2–9 | | 0.7 |
| $^{93}$Nb | 16 | ($n$,$n'$) | 2–7.5 | 2–7.5 | 14.6–22.7 | 0.6–0.78 |
| | 24 | ($n$,$n'$) | 4–7.0 | | 22.5–38.6 | 0.33–0.59 |
| $^{93}$Mo | 17 | ($p$,$n$) | 5.3 | ≤4 | 8.8 | 0.57 |
| | 18 | ($p$,$n$) | 7–13 | 3–8 | 11.4 | 0.7–0.86 |
| | 20 | ($p$,$n$) | 9–12 | 2–8 | 11 | 0.7–1.05 |
| | Present work | ($p$,$n$) | 7.8–14 | 2–8 | | 0.68 |
| Mo | 25 | ($n$,$n'$ + $2n$) | 14 | | 13.5 | 0.90 |
| | 27 | ($n$,$n'$ + $2n$) | 14 | | 10.2 | 1.02 |
| $^{181}$Ta | 16 | ($n$,$n'$) | 2–7.5 | 2–7.5 | 21.5–26.7 | ··· |
| | 23 | ($n$,$n'$) | 5–7 | 3–7 | 16.4–17.7 | 0.56–0.63 |
| | 26 | ($n$,$n'$ + $2n$) | 14 | | 23–27 | 0.82 |
| $^{181}$W | 19 | ($p$,$n$) | 8–10 | 3–7 | ··· | 0.64–0.78 |
| | 20 | ($p$,$n$) | 9–12 | 3–7 | 25 | 0.5–1.05 |
| | 21 | ($p$,$n$ + $2n$) | 18 | | | 1.04 |
| | Present work | ($p$,$n$) | 8–14.8 | 2–7 | ··· | 0.54 |
| W | 23 | ($n$,$n'$) | 5–7 | 3–7 | 16.0–16.6 | 0.52–0.6 |
| | 27 | ($n$,$n'$ + $2n$) | 14 | | 21.7 | 0.72 |

tained temperatures of 0.59, 0.52, and 0.5 MeV, respectively. In the case of Nb, however, the nuclear temperature was found to depend on bombarding energy, indicating that some nonequilibrium processes might have been present. Similar results have been reported by Owens and Towle, who obtain temperatures of about 0.55 MeV for both Ta and W, but find a dependence of temperature on bombarding energy as well. Level-density parameters for Mo and Ta have been obtained by Plattner *et al.* and Sobottka *et al.*, respectively, and those for Y, Mo, and W by Mathur *et al.* These data were obtained from 14-MeV neutron bombardment and extraction of the level-density parameters is complicated by the presence of $(n, 2n)$ neutrons. Temperatures of 0.9 for Mo and 0.82 for Ta were obtained in the first two experiments and values of 0.93, 1.02, and 0.72 for Y, Mo, and W, respectively, were obtained by Mathur *et al.* There is some indication[26] that use of the Lang and LeCouteur formula[21] yields level-density parameters for Ta which do not agree with those obtained by calculating the spectral shape directly; this might imply that the Lang and LeCouteur relation, which was derived for neutron cascades, is not an accurate representation of an $(n, 2n)$ spectrum.

### B. Reaction Mechanisms

The present measurements indicate that nonequilibrium processes are more easily observed for nuclei with $A$ near 90 and 180 than for nuclei near $A=55$. The lower temperatures characteristic of these nuclei produce a more rapid decrease in the equilibrium cross section to given final states as the bombarding energy is increased, with the result that nonequilibrium contributions can be observed more easily. Comparison of the present results with those of Ref. 1 indicates that the magnitude of the nonequilibrium contributions to the $(p, n)$ cross section varies only slightly between selected nuclei in the $A = 50$, $A = 90$, and $A = 180$ regions. Thus, the ratio $\Gamma_{con}/\Gamma_{int}$, where $\Gamma_{con}$ is the continuum width and $\Gamma_{int}$ the total width of the pre-equilibrium state, does not change significantly for the nuclei investigated. The total width $\Gamma_{int}$, however, does increase from about 160 keV to about 1 MeV between $A = 55$ and $A = 181$. Theoretically, this width is expected to be proportional to $g^3E^{*2}$, where $g$ is the single-particle level spacing and $E^*$ is the excitation energy. If $g$ is assumed to be proportional to $A$, this would result in a value of over 30 for the ratio $\Gamma_{int}(A = 181)/\Gamma_{int}(A = 55)$, while the experimental value is 6.

Application of the level-density formulas obtained from the assumption of a constant single-particle level spacing leads to the prediction that the nonequilibrium spectrum will have a linear dependence on $U$ for both the direct and pre-equilibrium portions of the $(p, n)$ spectrum. Disagreement with this prediction was observed for the reactions $^{51}V(p, n)^{51}Cr$ and $^{59}Co(p, n)^{59}Ni$, for which a quadratic dependence on $U$ produced the best fit to the data. This discrepancy was not regarded as serious, because of (1) the uncertainty of one unit in the $n$ determination procedure, and (2) small contributions from higher-order terms in the series. The present measurements especially $Nb(p, n)$ show much larger disagreements with theoretical predictions and are too large to be explained by the above factors. A more probable explanation is that because of shell effects, the single-particle level spacing is not sufficiently independent of excitation energy to be regarded as constant. The basic assumption of the model is that the relevant residual states are one-particle (proton)–one-hole (neutron) states. Such a level density would be expected to show the effects of non-uniform single-particle level spacing more dramatically than would the total level density which includes all configurations. Since the effect of shells is to produce large gaps between ground or low-lying states and higher excited states, the result is to reduce the rate of increase in level density for small values of $U$ relative to that for higher $U$; this effect of a gap would be in the proper direction to cause the "best-fit" value of $n$ to be larger than it would be in the absence of shell effects. Similar behavior in the neighborhood of closed shells has been noted by Cline and Blann.[28] Calculations by Maruyama[16] also have shown that shell effects would be more obvious in the constituent level densities (e.g. proton particle states) than in the composite level densities. It is clear that measurements for a number of nuclei near closed shells will be necessary to determine whether this behavior is characteristic of nuclei near closed shells or unique to the nuclei studied here.

## VI. SUMMARY

Examination of the neutron spectra from $(p, n)$ reactions on $^{89}Y$, $^{93}Nb$, and $^{181}Ta$ has shown that substantial contributions from nonequilibrium processes are present for bombarding energies above 10 MeV. Data obtained at lower energies were used to obtain the level-density parameters for $^{89}Zr$, $^{93}Mo$, and $^{181}W$; a constant-temperature form is found to be appropriate for energies below the neutron binding energy, with temperatures of 0.7, 0.68, and 0.54 MeV, respectively.

Spectra at higher bombarding energies were resolved into equilibrium and nonequilibrium portions. Use of the bombarding-energy dependence

of the compound-nuclear portion enabled the level-density measurements to be extended to about 12 MeV. Changes in temperature consistent with the expected transition to a Fermi-gas level-density form were observed above 10 MeV.

The characteristics of the nonequilibrium part of the spectrum were found to be in basic agreement with the predictions of the current model. Inconsistencies in the residual excitation-energy dependence of the spectra were observed and tentatively attributed to shell effects.

Comparison of the magnitudes of the equilibrium and nonequilibrium cross section provided an estimate of the intermediate-state width and that fraction of the width corresponding to particle emission. The widths varied between approximately 300 keV for $^{90}$Zr and $^{94}$Mo to 1 MeV for $^{182}$W; the width for nonequilibrium particle emission was found to be between 5 and 10% of the total width of these states.

---

†Work performed under the auspices of the U. S. Atomic Energy Commission.

[1]S. M. Grimes, J. D. Anderson, J. W. McClure, B. A. Pohl, and C. Wong, Phys. Rev. C 3, 645 (1971).

[2]J. J. Griffin, Phys. Rev. Letters 17, 478 (1966).

[3]M. Blann, Phys. Rev. Letters 21, 1357 (1968).

[4]F. C. Williams, Jr., Phys. Letters 31B, 184 (1970).

[5]V. F. Weisskopf, Phys. Rev. 52, 295 (1937).

[6]V. A. Sidorov, Nucl. Phys. 35, 253 (1962).

[7]R. M. Wood, R. R. Borchers, and H. H. Barschall, Nucl. Phys. 71, 529 (1965).

[8]H. Feshbach, A. K. Kerman, and R. H. Lemmer, Ann. Phys. (N.Y.) 41, 230 (1967).

[9]The factor $(2S+1)$ was inadvertently omitted from the corresponding equation in Ref. 1.

[10]J. D. Anderson and C. Wong, Nucl. Instr. Methods 15, 178 (1962); B. D. Walker, J. D. Anderson, J. W. McClure, and C. Wong, *ibid.* 29, 333 (1964).

[11]T. Ericson, and V. Strutinski, Nucl. Phys. 8, 284 (1958).

[12]T. Ericson, Advan. Phys. 9, 425 (1960).

[13]V. F. Weisskopf and D. H. Ewing, Phys. Rev. 57, 472 (1940).

[14]F. D. Becchetti and G. W. Greenlees, Phys. Rev. 182, 1190 (1969).

[15]P. E. Hodgson, in *Proceedings of the International Conference on Direct Interactions and Nuclear Reaction Mechanisms, Padua, Italy, 1962,* edited by E. Clementel and C. Villi (Gordon and Breach, Science Publishers, Inc., New York, 1963), p. 103.

[16]M. Maruyama, Nucl. Phys. A131, 145 (1969).

[17]R. L. Bramblett and T. W. Bonner, Nucl. Phys. 20, 395 (1960).

[18]C. Wong, J. D. Anderson, J. W. McClure, and B. D. Walker, Nucl. Phys. 57, 515 (1964).

[19]C. H. Holbrow and H. H. Barschall, Nucl. Phys. 42, 264 (1963).

[20]R. R. Borchers, R. M. Wood, and C. H. Holbrow, Nucl. Phys. 88, 689 (1966).

[21]V. V. Verbinski and W. R. Burrus, Phys. Rev. 177, 1671 (1969).

[22]K. J. LeCouteur and D. W. Lang, Nucl. Phys. 13, 32 (1959).

[23]R. O. Owens and J. H. Towle, Nucl. Phys. A112, 337 (1968).

[24]D. B. Thompson, Phys. Rev. 129, 1649 (1963).

[25]R. Plattner, P. Huber, C. Poppelbaum, and R. Wagner, Helv. Phys. Acta 36, 1059 (1963); P. Huber, R. Plattner, C. Poppelbaum, and R. Wagner, Phys. Letters 5, 202 (1963).

[26]H. Sobottka, S. Grimes, P. Huber, E. Mangold, J. Schacher, and R. Wagner, Helv. Phys. Acta 43, 559 (1970).

[27]S. C. Mathur, P. S. Buchanan, and I. L. Morgan, Phys. Rev. 186, 1038 (1969).

[28]C. K. Cline and M. Blann, University of Rochester Report No. UR 3591–17, 1971 (unpublished).